Journal of Metals, Materials and Minerals, Vol.23 No.2 pp.9-22, 2013

Fabrication of chitosan/titanium dioxide composites film for the photocatalytic degradation of dye

Parichat NORRANATTRAKUL[1], Krisana SIRALERTMUKUL[2] and Roongkan NUISIN[3*]

[1]Inter-Department of Environmental Science, Graduate School,
Chulalongkorn University, Bangkok, Thailand.
[2]The Metallurgy and Materials Research Institute, Chulalongkorn University, Bangkok, Thailand.
[3]Department of Environmental Science, Faculty of Science, Chulalongkorn University, Bangkok, Thailand.

Abstract

The investigation of the chitosan film as a polymer matrix for titanium dioxide (TiO_2) dispersion was carried out. Chitosan–titanium dioxide composite films were prepared by solution casting, using Chitosan, TiO_2, Arquad T50 HFP as surfactant. The mixture of 1.0 g chitosan in 100 mL acetic acid was prepared, subsequently with the addition of TiO_2. The solution was then cast onto an acrylic mold and allowed to air-dry. The external morphology of the composite film revealed the high dispersion of TiO_2 in the polymer matrix. Three types of crosslinking agent; glutaraldehyde, citric acid, and itaconic acid were studied. It was found that chitosan film crosslinked with 1.12 mM citric acid for 5 min exhibited the highest tensile strength about 150.4 MPa. X-ray diffraction patterns of the dried film revealed the minor change in the theta of the crystalline region of chitosan. The diffraction line shift was likely due to the change in its chain orientation caused by the covalent interactions between chitosan and the crosslinking agent. The non-crosslinked chitosan-TiO_2 composite film exhibited the higher tensile stress at maximum load with TiO_2 content of 1 wt%, whereas the high content of TiO_2 revealed the poor tensile stress at maximum load due to an aggregation of nanoparticles. The spent film for dye removal had the lower tensile stress at maximum load than that of the original film. Three reactive dyes of RR 120, RY 17, and RB 220 were selected as a representative contaminant. The optimal TiO_2 amount for dye removal in both UV and dark conditions was 1 wt.% of chitosan. The chitosan-TiO_2 composite films without crosslinking had the higher efficiency in dye removal than the crosslinked films. Dye removal in UV condition had the higher efficiency than without UV for all initial dyes concentrations in the range of 10 to 100 $mg{\cdot}L^{-1}$. The ratio of sorption to photocatalysis of RR120, RY17, and RB220 were 70.7:29.3, 78.5:21.5, and 92.2:7.8, respectively. Langmuir isotherm was used for data analysis for dark condition and the results showed that q_{max} of RR120, RY17, and RB220 were 46.8, 427.1, and 229.1 mg-dye$\cdot g^{-1}$-chitosan-TiO_2 film, respectively. The analysis of dye removal in UV condition followed satisfactorilly a Langmuir-Hinshelwood model in dye removal efficiencies. This indicated that photocatalysis process occurred on the surface of TiO_2 and in the solution.

Introduction

Chitosan (2-acetamido- 2-deoxy-β-D-glucose) is a cationic biopolymer obtained from crustacean such as shrimps and crab shells and produced by the N-deacetylation of chitin, the second most abundant natural polymer. The structure of chitosan were glucosamine unit linkage with β-(1,4) bonds.(1) In addition, the chitosan molecules contain a large number of relative hydroxyl (OH) and amine (NH_2) groups, which can easily attach ligands.(2) A portion of chitosan undergoes extensive crosslinking to yield modified chitosan whose properties are different from those of native chitosan.(3) Polymer crosslinking leads to the formation of a permanent covalent network, which may allow the free diffusion of water/ bioactive materials and also enhance a mechanical properties of a polymer. The antimicrobial, biocompatible, and biodegradable properties of chitosan make these films ideal candidates for the applications on polymeric film, protective food coating, controlled released drug carrier.(4-7) In view of its hydrophilicity, excellent film-forming ability, good mechanical properties, and high chemical reactivity, chitosan can be an excellent candidate for affinity membranes. Until now, chitosan membranes have been used for active films in food area(8-9) pervaporation(10), and ultrafiltration.(11-12)

Inorganic particles are well known to enhance the mechanical and tribological properties of polymers, and this issue has been widely investigated.(13-14) Reducing the particle size to a

*Corresponding author E-mail : Roongkan.N@Chula.ac.th

nano-scale level is suggested to improve significantly the composite efficiency; nanoparticle -filled polymers, the so-called polymer nanocomposites, are very promising materials for various applications.[15] For practical applications, the photocatalyst should be immobilized to provide flat surfaces that receive sunlight or artificial light. TiO_2 is a nanoparticles and a fascinating material from a surface science point of view.[16] The thin films of TiO_2 can be directly prepared on various substrates by sputtering, electrolytic oxidation of titanium plates, diping, spinning, spray coating of titanium compounds, and sol-gel method.[17] However, the photocatalytic activity of these films is much lower than that of fine powder TiO_2 catalysts. Photocatalytic performance is very much improved by using finer TiO_2 particles, increasing TiO_2 content and making porous structures.[18] The combination of TiO_2 photocatalysis and polymeric membrane of chitosan have an advantage on wastewater treatment. The membrane has a capability to retain the photocatalysis, and the pollutants are oxidized by the photocatalysis.

In the present study, titanium dioxide nanoparticles were immobilized into chitosan solution subsequently with casting method. The objectives of this study were determined the physical properties of chitosan with and without the addition of TiO_2. The effects of an amount of TiO_2 on tensile strength were examined. In addition, the effects of three type of crosskinging agent on chitosan film properties, namely glutaraldehyde, citric acid, and itaconic acid were also revealed.

Experimental part

Materials

Chitosan (Commercial grade, Biolife Co. Ltd., Bangkok, Thailand), shrimp shell obtained with degree of deacetylation (DD) of 81%, and an average molecular weight of 200,000 kDa was used. Exactly 1.0 g of chitosan was weighed and dissolved in 1 w/v% of 100 cm^3 acetic acid (analytical grade, Carlo Erba, Italy) by shaken at 1300 rpm for 24 hrs. The chitosan solution was filtered to remove the undissolved chitosan flake and the supernatant was collected. An anatase form of titanium dioxide (TiO_2) (Pharmaceutical grade, Sun Chemicals, Bangkok, Thailand) with surface area of 5.0219 $m^2.g^{-1}$, particle mass density of 2.4288×10^{-3} $g{\cdot}cm^{-3}$ was used. TiO_2 was sieved using 200 mesh and dried in oven at 60°C for 24 hr prior to used. TiO_2 with average particle size of 105.8 nm was measured. The TiO_2 nanosized were then added, to obtained 1 wt% of nanoparticle with the use of 5 wt% of glycerol (analytical grade, Carlo Erba, Italy) as plasticizer. The Arquad T-50 HFP (Tallowtrimethylammonium chloride or alkyltrimethyl ammonium chloride, analytical grade, Akzo Nobel Chemicals, Sweden) was used as steric detergent.

Chitosan-TiO_2 composite film preparation

The chitosan-TiO_2 composite films were prepared by solution casting method. The TiO_2 particles were added into chitosan solution, subsequent with homogenized at 1200 rpm to allow the homogeneously dispersed of TiO_2. The chitosan-TiO_2 solution was left until bubble free for 20 min. Then, the mixture was casted onto an acrylic sheet mold with a dimension of 100 mm × 100 mm, a wet thickness of 0.3 mm. The chitosan-TiO_2 film was obtained. The chitosan-TiO_2 cast film was then dried overnight in an air-dry. After the water completely evaporated, the films were carefully removed from an acrylic mold. The chitosan-TiO_2 films were conditioned by neutralizing with 1% NaOH solution (concentration of 7 $g{\cdot}cm^{-3}$). Then, the film was carefully rinsed and soaked with distilled water to remove the residual NaOH. The film was dried in a thermostat oven at 50°C for 24 hrs before the testing method was carried out. Crosslinking agents, namely glutaraldehyde (GA) or 1,5-pentanedial (analytical grade, Fluka, Germany), citric acid monohydrate or 1,2,3-propanetric carboxylic acid (CA) (analytical grade, J.T. Baker Chemicals, USA), itaconic acid (IA) (analytical grade, Acros Organics, Belgium) was used as received.

Characterizations

Physical property measurement

The thickness of the chitosan film was measured with a Vernier caliper. However, this type of measurement was not very precise since the amount of pressure applied by the operator's thumb cannot be quantified or reproduced precisely. Hence, the readings may vary from operator to operator.

Tensile strength

The tensile strength of chitosan-TiO_2 was measured with a Universal testing machine (LLoyd model 100 LR, England). The synthesized chitosan-TiO_2 was cut into slices with a dimension of 25 mm × 70 mm. The composite specimens were characterized for their tensile and flexural properties in the longitudinal direction in accordance with ASTM D882-83 type E (constant-rate-of-extension). Tensile test specimens with a dimension of 5 mm × 65 mm were used with the thickness of 0.030 ±0.002 mm for chitosan film, and the thickness of 0.05 ± 0.002 mm for chitosan-TiO_2 film. These specimens were all tested at a gauge length of 50 mm. The tests were carried out using a load cell of 25 mm in length. Tensile and flexural tests were performed at a crosshead speed of 25 mm·min^{-1} (strain rate of 1 min^{-1}) and 2 mm·min^{-1}, respectively.

Swelling property

Swelling behavior of the chitosan film crosslinked with citric acid (CA) and the chitosan film loaded with 1 wt% TiO_2 was studied. The dry weight (w_1) of each sample was measured with an analytical balance. The sample was immersed in distilled water with a pH of 5.5 at the time interval of 1, 3, 5, and 7 days. Then, the sample was taken out and the excess water on its surface was wiped with a filter paper. The swollen films were eventually weighed. The degree of swelling for each sample at time t was calculated by using the following expression (1):

$$Swelling\ (\%) = [(w_2-w_1)/w_1] \times 100 \quad (1)$$

where w_2 are the weights of the films at time t

Scanning electron microscopy

The external morphology of chitosan-TiO_2 film was investigated using Scanning Electron Microscopy (SEM) (Philips, model XL 30CP, USA). The films were cut and mounted on a brass stubs with double-sided adhesive tape and were coated with 50 A° of gold vapor with an SCD-040 Balzers sputter. The specimen was finally characterized by SEM using and accelerating voltage of 15 kV, and a 1000× magnification of the original specimen size.

X-ray diffraction

X-ray Diffraction (XRD) was employed for the crystallinity of the polymer. X-ray diffraction was performed using a Philips model PW 3710 (Philips, USA) diffractometer with CuKα radiation (λ = 0.1542 nm) in sealed tube operated at 40 kV and 30 mA. The diffraction patterns were obtained from 2 to 40 2-theta degree with a scanning rate 1 min^{-1}. The basal spacing of the silicate layer, d, was calculated using Bragg's equation, $k = 2d\sin\theta$ (where θ is the diffraction position and k is the wavelength). The scan speed ($2\theta \cdot s^{-1}$) of 0.040 s^{-1} was used.

Functional group of composite films

The Attenuated Total Reflection Fourier Transform Infrared Spectroscopy (ATR-FTIR) Perkin Elmer model 1760X (Perkin Elmer, USA) was used for characterizing the functional groups of the composite film. The ATR-FTIR spectra were recorded at room temperature. For each spectrum, 128 scan cycles were averaged; in each cycle, the ratio of the sample spectra with respect to the background spectra of a clean germanium plate was measured, using a shuttle to move the sample or reference into the beam. For polarization experiments, a Perkin-Elmer gold wire grid polarizer was positioned before the sample and the reference.

Adsorption experiments

Adsorption equilibrium was determined by the batch method for 500 mL of dye solution. The initial concentration of dyes, namely RR 120, RY 17, and RB 220 were 10, 25, 50, 75, and 100 mg.L^{-1} at pH 9. The beakers were placed in a control temperature at 25±2ºC in dark room. Dye removal efficiency was determined spectrophotometrically (UV-Visible spectrophotometer, model G1103A, Agilent, USA) by sampling 5 mL of the solution for 360 minutes. The passage of the sample was examine 3 times separately under dark and UV light conditions.

Results and discussion

Effect of TiO_2 contents on crystallinity of chitosan /TiO_2 films

X-ray diffraction (XRD) is an effective method for the investigation of the crystalline

region of chitosan and the existence of TiO_2. The wide angle X-ray diffraction patterns of TiO_2 anatase and chitosan in the region between 2 to 80 degrees 2θ are shown in Figure 1f and 1a, respectively. The x-ray diffraction pattern for anatase phase TiO_2 (1 1 0) shows single diffraction lines at 25.0, 38.22, 48.22, and 54.54 degrees 2θ (Figure 1f). Similarly, Zainal *et al.* (2005)[19] reported the XRD patterns at 25.28, 17.80, and 40.25 degrees 2θ, respectively. The crystalline structure of chitosan shows diffraction lines at 9.39, 15.43, and 20.63 degrees 2θ (Figure 1a). Figure 1b to 1d shows the XRD pattern of the chitosan-TiO_2 with the amount of TiO_2 content varied from 0.5, 1, 3, and 5 wt% of chitosan. It was found that the intensity of the diffraction lines at 15.43° 2θ degree decreased and revealed the diffraction lines at 25 degree 2θ corresponding to TiO_2. The XRD pattern of the film shows the increasing of intensity of TiO_2 region corresponding to the amount of TiO_2 loaded. This phenomenon was likely to be due to the increase of amorphous region in chitosan matrix occurring during the component blending.

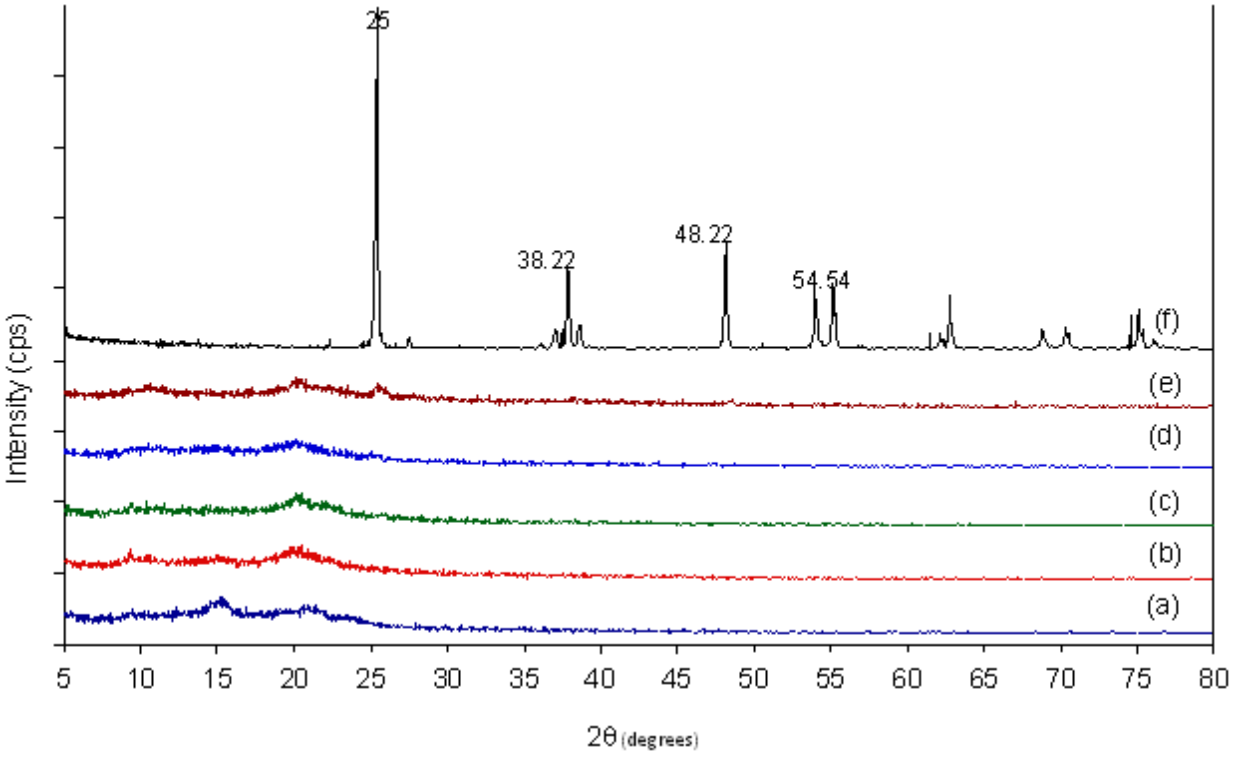

Figure 1. X-ray diffraction patterns of (a) native chitosan, (b) chitosan with 0.5 wt% TiO_2, (c) chitosan with 1 wt% TiO_2, (d) chitosan with 3 wt% TiO_2, (e) chitosan with 5 wt% TiO_2, and (f) anatase form of TiO_2

Effect of crosslinking agent on chitosan and chitosan/TiO_2 films

The composition of chitosan films was crosslinked with three types of crosslinking agent, namely glutaraldehyde (GA), citric acid (CA), and itaconic acid (IA). For those using the GA, the reaction occurs through a Schiff's base reaction between aldehyde groups of GA and some amine groups of chitosan, but the links with hydroxyl groups of chitosan cannot be excluded.[20] Itaconic acid is a dicarboxylic structure. The possibly structure of chitosan film crosslinked with CA is reported by Pena *et al.*, (2006).[21] It is the key factor on finding a precursor solution from which both forms could be obtained. Citric acid is a tricarboxylic structure. In this sense, Citric acid is a tricarboxylic structure: it allows to dissolved chitosan and, due to its chelating nature. In addition, CA along with chitosan facilitates the formation of layers due to its properties as film former, attributable to its ability to enhance gelation improving the wettability of a coating solution on a substrate. The possibly structure of chitosan film crosslinked with CA was reviewed.[22]

Chitosan film was neutralized and crosslinked with various concentration of citric acid at 0.56, 1.12, and 1.68 mM. The XRD pattern of the non-crosslinked chitosan film revealed the peaks at 9.39, 15.43, and 20.63 degrees 2θ (Figure 2a). Depending on the origin of the polymer and its treatment during the extraction from raw material, the residual crystallinity may vary considerably.[2] The reduced polymer crystallinity can be occurred through the crosslinking reaction. The hydrogen bond between polymer chains from the two functional groups of $–NH_2$ and –OH was broken due to the crosslinking interaction of –COOH group from citric acid. Then, the amorphous region of polymer was increased.[23] This crosslink was found to reduce the dissolution of polymer in the solution.[20] It was found that the 0.56 and 1.12 nM of citric acid, the lines at 9.42, 15.43, and 21.22 degrees 2θ as shown in Figure 2b and at 9.42, 9.22, and 20.90 degrees 2θ (Figure 2c), respectively. While, for the concentration of 1.68 mM, the crystallinity was slightly shifted as shown by the diffraction lines at 9.30, 14.86, and 20.66 degrees 2θ (Figure 2d). The crosslinking network of polymer was increased and the amorphous region of polymer was enhanced due to the high concentration of CA.

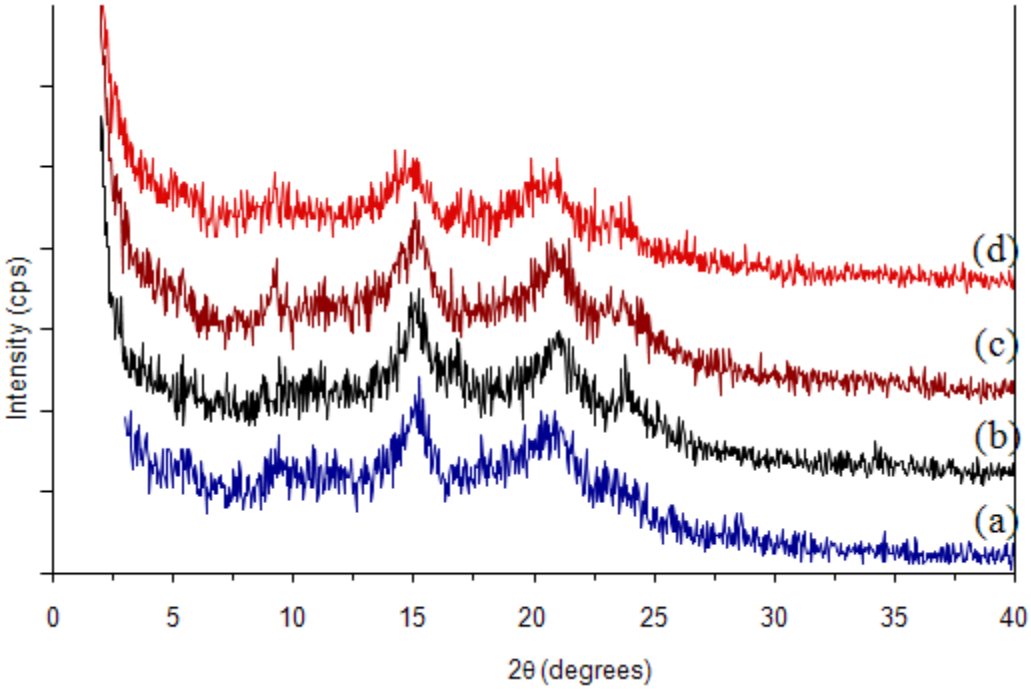

Figure 2. XRD patterns of (a) non-crosslinked chitosan film and crosslinked chitosan films prepared from (b) 0.56 mM (c) 1.12 mM (d) 1.68 mM of citric acid

Effect of TiO_2 on external morphology of chitosan/TiO_2 films

Surface morphology of chitosan-TiO_2 films under scanning electron microscopy (JEOL scanning electron microscope) was carried out in order to investigate the TiO_2 dispersion in the chitosan matrix. The external morphology of the native chitosan films revealed the smooth and flatten surface as shown in Figure 3a in comparison with the microscopic surface of the chitosan films containing 1 wt% TiO_2 (Figure 3b), 3 wt% (Figure 3c), and 5 wt% (Figure 3d). The TiO_2 particles were aggregated in the chitosan matrix as the content of TiO_2 loading was higher. The bright area on the image and the rough surface was observed. It could be seen that, the chitosan film containing 5 wt% of TiO_2 exhibited the large cluster size of aggregated TiO_2 particle of about 5 mm. The poor distribution of TiO_2 particles in the chitosan film is most likely caused by the lack of attractive forces between chitosan and TiO_2. Typically, there is no attractive force between chitosan and TiO_2. It was expected that the finer TiO_2 dispersion, in the case of adding surfactant, in the chitosan matrix could act as a dispersing agent for TiO_2 particles in chitosan solution.

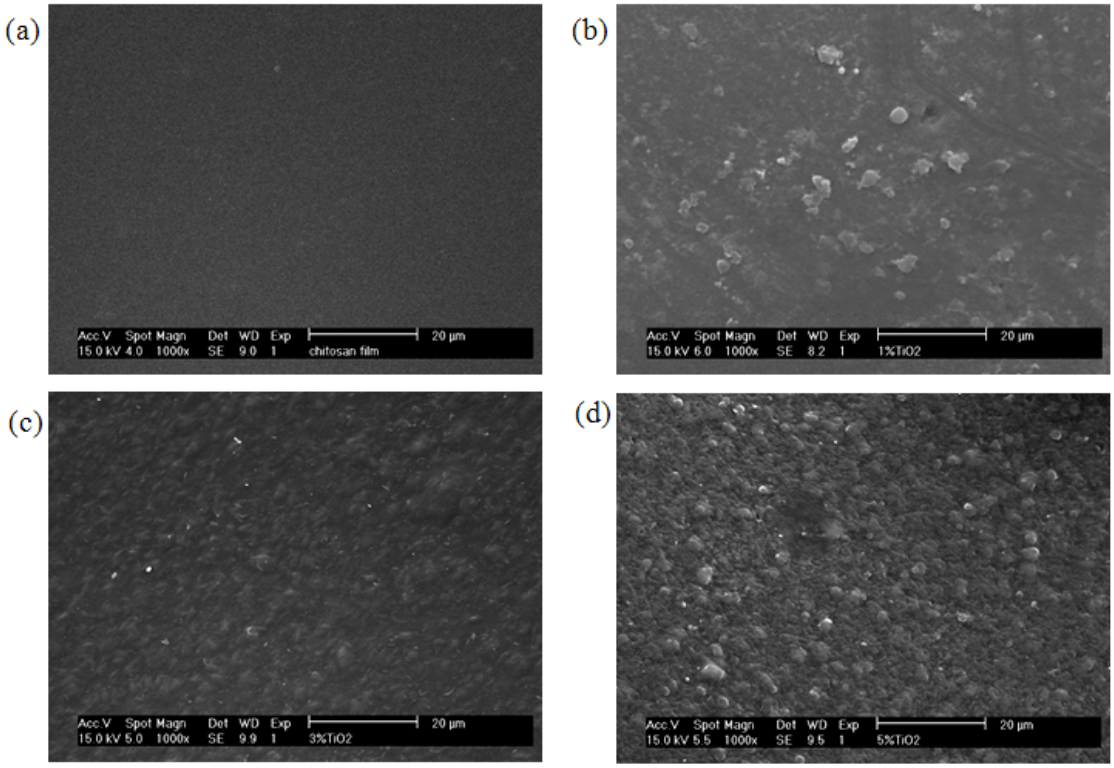

Figure 3. Scanning electron micrographs showing the surface morphology of the chitosan film with various TiO_2 loading; (a) native chitosan, (b) 1 wt%, (c) 3 wt%, and (d) 5 wt% of TiO_2.

Tensile properties of chitosan-TiO_2 composite film

The various amount of TiO_2 of 0.5, 1.3, 3, and 5 wt% of chitosan was conventionally added into chitosan solution. The air-dry chitosan-TiO_2 film was subsequently crosslinked with 1.12 mM of citric acid. It was found that addition of TiO_2 nanocomposite into the chitosan film could enhance the physical properties and mechanical properties of the film. The non-crosslinked chitosan film revealed the tensile stress at maximum load at 44.1 MPa. As the amount of TiO_2 was increased, the tensile modulus was decreased. The tensile stress at maximum load values was found to be 41.7, 49.5, 21.2, and 14.8, respectively as shown in Fig. 4. Whereas, the tensile stress at maximum load of chitosan-TiO_2 when the film was crosslinked was found when the 1.12 mM of citric acid was employed. It was found that the tensile stress at maximum load was decreased. The values turned out to be 37.39, 32.31, 17.34, and 16.26, respectively. As the TiO_2 content was increased, the high particle content was found to induce the agglomeration of the chitosan matrix due to an adhesive force as shown in Figure 3. We anticipate that the interactions between the TiO_2 surfaces and chitosan molecules could be the van der Waals force, which is weaker that of the interactions between the chitosan-chitosan molecules. The phase separation was occurred between solid phase of TiO_2 and chitosan matrix. Therefore, the higher TiO_2 can be considered as some kind of molecular spacer which prevent the homogeneously dispersion in polymer matrix, thus results in the low tensile stress at maximum load value.

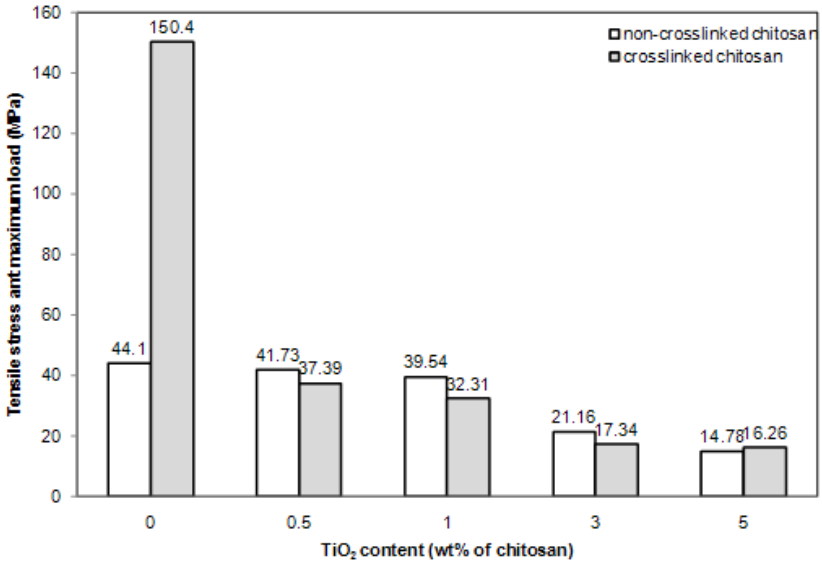

Figure 4. Effect of TiO_2 contents on tensile stress at maximum load of chitosan films

Effect of TiO_2 contents on swelling properties

The swelling behavior of the chitosan-TiO_2 films with 1 wt.% TiO_2 loading in distilled water of pH 7 at ambient temperature is shown in Figure 6. On keen observation of the plot, the character of swelling curves changes over time. The swelling was found to reach a stable equilibrium at 5 days. It was also observed that the swelling curve of non-crosslinked chitosan changed greatly as compared to that of the crosslinked films. The addition of 1 wt% TiO_2 into chitosan film caused in the swelling curved to decline. By comparing among the prepared chitosan-TiO_2 films, the 1 wt% TiO_2 crosslinked with CA resulted in the lowest degree of swelling. This suggests that the dispersion of particle into polymeric film can cause the film to exceed the swelling degree in some extent as shown in Figure 5.

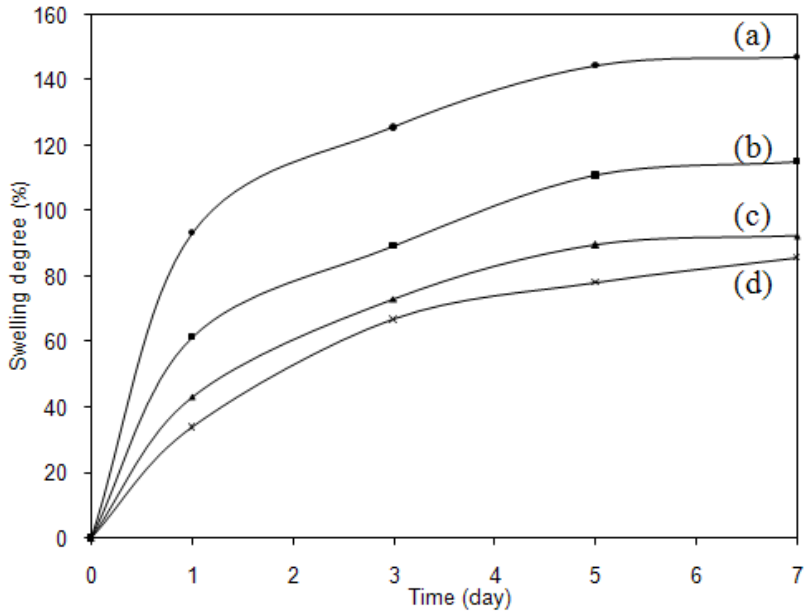

Figure 5. Effect of TiO_2 content on swelling behavior of chitosan film at various interval time; 0,1, 3, 5, and 7 days, pH 5.5 at room temperature for (a) non-crosslinked chitosan, (b) chitosan crosslinked with CA, (c) non-crosslinked chitosan-TiO_2, and (d) chitosan-TiO_2 crosslinked with CA.

Effect of crosslinking agents on swelling content

As shown in Fig. 6, the swelling capabilities of the chitosan film increased with time, reaching a constant swelling (equilibrium swelling) after a certain period of time. The incorporation of CA into the polymer network at higher CA content lead to an increase in electrostatic repulsive forces between the charged sites of carboxylate ions upon their complete dissociation, thus enhance the more extended configuration. The extended structure with high-CA content resulted in the swelling of the chitosan film in water. Since CA is a tricarboxylic acid, the higher swelling degree was expected as compared to that of the dicarboxylic one.[24] Using glutaraldehyde, the lowest swelling degree was eventually obtained.

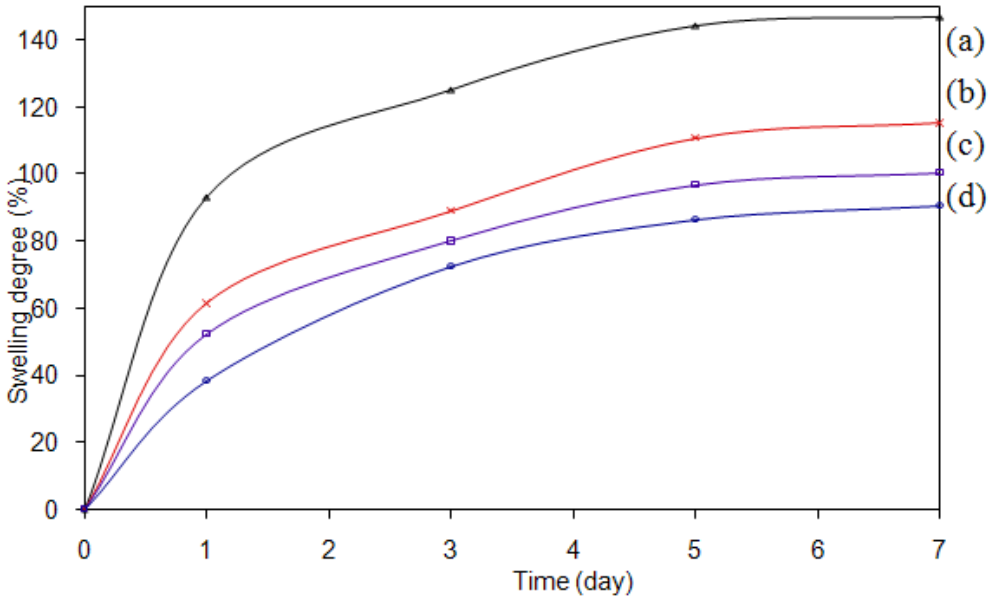

Figure 6. Effect of crosslink agent types on swelling behavior of (a) non-crosslinked chitosan film and chitosan film crosslinked with (b) CA, (c) IA, and (d) GA.

Attenuated Total Reflection Fourier Transform Infrared Spectroscopy (ATR/FTIR)

Non-crosslinked and crosslinked chitosan film with 1.68 mM of GA, CA, and IA for 20 minutes was prepared and characterized using ATR-FTIR techniques. ATR/FTIR results (Figure 7) show peaks around 905 cm^{-1} and 1150 cm^{-1} corresponding to the saccharide structure.[22] The peaks of amide II were found in the range of 1577-1515 cm^{-1}. There were also two absorption peaks at 1648 cm^{-1} and 1319 cm^{-1}, corresponding to the chitin and chitosan vibrational frequencies. These two peaks were reported as amide I and III. The sharp peaks at 1383 cm^{-1} and 1420 cm^{-1} were assigned to the CH_3 symmetrical deformation mode. The broad peak at 1083 cm^{-1} indicated the C—O stretching vibration in chitosan. Another broad peak in the region of 3750-3000 cm^{-1} was likely due to amine N—H symmetrical vibration (broad, s). Peaks at 2900 cm^{-1} and 2850 cm^{-1} are the typical C—H stretch vibrations (m).

The significant peak was found at 1631 cm^{-1}, corresponding to the formation of imine bond (C=N) in Schiff's base structure by the reaction between amino groups of chitosan and aldehyde groups of glutaraldehyde (Figure 8b).[22] A significant peak at 1577 cm^{-1} was also observed. Because of the instability of the imine bond (C=N) of the Schiff's structure, the hydrogen could undergo structural changes depending on the reactant structure, temperature, and pH of the solution. The characteristic peaks of these products appeared around 1190-1140 cm^{-1}, 1100- 1060 cm^{-1} and 1060-1035 cm^{-1}, suggesting the cross-linking reaction between the chitosan molecules. The mechanism of this cross-linking reaction was schematically illustrated in Wang *et al.*, (2004).[22] In the case of crosslinked chitosan with other acid e.g. citric and itaconic acid, the strong peak of the COO- group at 1626-1540 cm^{-1} was observed as showed in Figure 8 (c, and d). It is therefore confirmed that citric acid and itaconic acid were crosslinked to the chitosan. The spectra of polymeric films were shown in Figure 7.

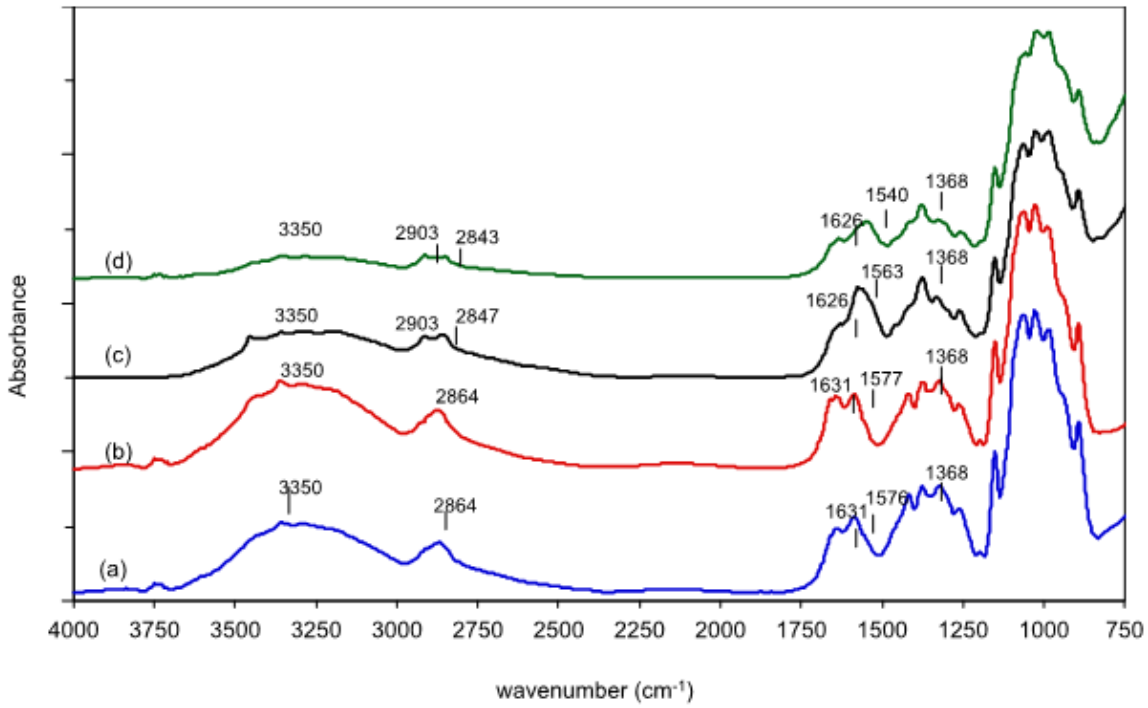

Figure. 7. ATR/FTIR spectra of chitosan (a) non-crosslinked; crosslinked with (b) GA, (c) CA, and (d) IA, respectively.

Dye removal performance of chitosan-TiO_2 films

The adsorption experiments were carried out at pH 9 under dark (without UV) and UV light. Effect of chitosan-TiO_2 films on dye removal for various type and concentration of reactive dye namely; reactive red 120 (RR 120), reactive yellow 17 (RY 17), and reactive blue 220 (RB 220) as shown in Figure 9 a-c (opaque lines). The kinetics of dark adsorption of dyes on titanium dioxide supported on the chitosan films are represented the Langmuir adsorption model. The Langmuir equation assumes that there is no interaction between the sorbate molecules and that the sorption is localized in a monolayer. Then, assumed that once a dye molecules occupies a site no further sorption can take place. The Langmuir equation are given as eq. 2, where C_e is the equilibrium concentration of dyes in solution ($mg.L^{-1}$), x/m is the amount of dye sorbed per unit of sorbent ($mg.g^{-1}$, "a" is a constant related to the area occupied by a monolayer of sorbate, reflecting the sorption capacity ($mg.g^{-1}$), "b" is a direct measure for the intensity of the sorption process ($l.mg^{-1}$).[25] Besides, the results of dye decolorization under the UV/Vis irradiation was observed (Figure 9 a-c). The efficiency of dyes reduction increasing with the photocatalysis on the surface of TiO_2.

The photocatalytic reaction of dyes over titanium dioxide had obeyed the Langmuir-Hinshelwood mechanism as shown in equation 3.[26] The "b" from Table 1 was used for calculation. The integration of equation 1 with condition of $t=0 \rightarrow C = C_0$, the equation 3 and 4 was given. The plot of $(1/b)\ln(C_o/C_t) + (C_o–C_t)$ versus time (t) shows a linear variation as shown in Figure 10 (a-c). The slope of the straight line from origin is r_{max}. The values of $\ln(C_0/C_t)$ at different initial dye concentration were linear variation (equation 5). Where, C_t is the concentration of the dye in the solution at time t. The regression coefficients are list in Table 2. The RB17 provide the better agreement with the Langmuir-Hinshelwood model, the degradation rate increases with the initial dye concentration as shown in Figure 10b. It was possibly related to the molecular size of the RB17 smaller than that of other. A tendency of degradation revealed independent values with the initial concentration. The RR 120 and RB 220, the increasing of initial concentration, the higher degradation was obtained. In comparison, the ratio of sorption to photocatalysis of RR120, RY17, and RB220 were 70.7:29.3, 78.5:21.5, and 92.2:7.8, respectively.

$$q = \frac{x}{m} = \frac{q_m b C_e}{1 + b C_e} \tag{2}$$

$$r = -\frac{dC}{dt} = \frac{r_{\max} bC}{1 + bC} \tag{3}$$

$$\int_{C_o}^{C_t} \frac{1 + bC}{r_{\max} bC} dC = -\int_o^t dt \tag{4}$$

$$(1/b)\ln(C_o/C_t) + (C_o - C_t) = r_{\max}\, t \tag{5}$$

Table 1 Langmiur adsorption constants

Dyes	q_m (mg.g^{-1})	b (L.mg^{-1})	R^2
RR 120	46.8	0.0720	0.877
RY 17	427.1	0.0071	0.982
RB 220	229.2	0.1969	0.673

Table 2 Pseudo-first order (Langmuir- Hinshelwood model) apparent constant values for the different concentration of dyes

C_0 (mg. L^{-1})	RR 120		RY 17		RB 220	
	$r_{\max}$ (mg.L^{-1}. min^{-1})	R^2	r_{max} (mg.L^{-1}. min^{-1})	R^2	r_{max} (mg.L^{-1}. min^{-1})	R^2
10	0.214	0.849	1.1250	0.9324	0.1323	0.7797
25	0.240	0.892	0.7974	0.9214	0.1953	0.8527
50	0.483	0.889	1.3462	0.9644	0.2986	0.8732
75	0.328	0.896	1.0244	0.9390	0.4003	0.8692
100	0.347	0.896	0.9693	0.9635	0.3913	0.9074

(a)

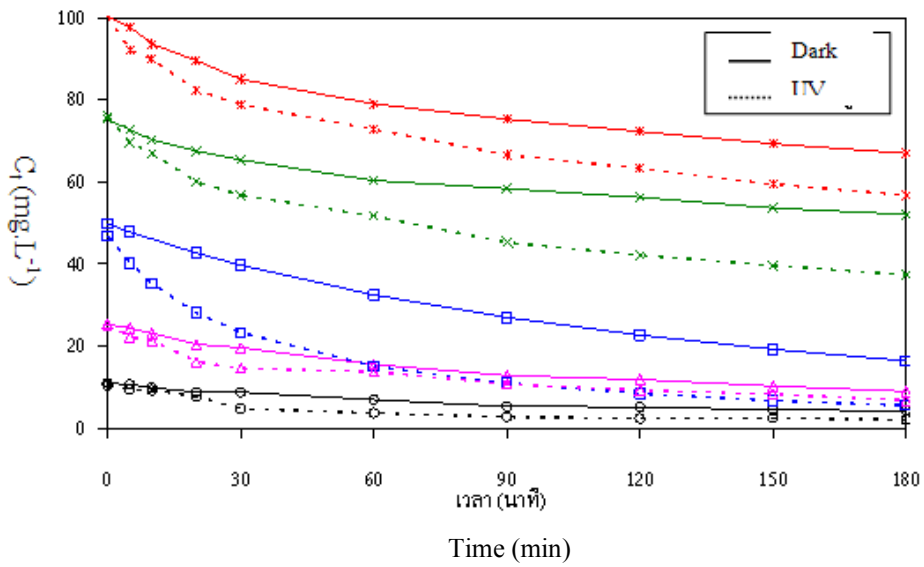

(b)

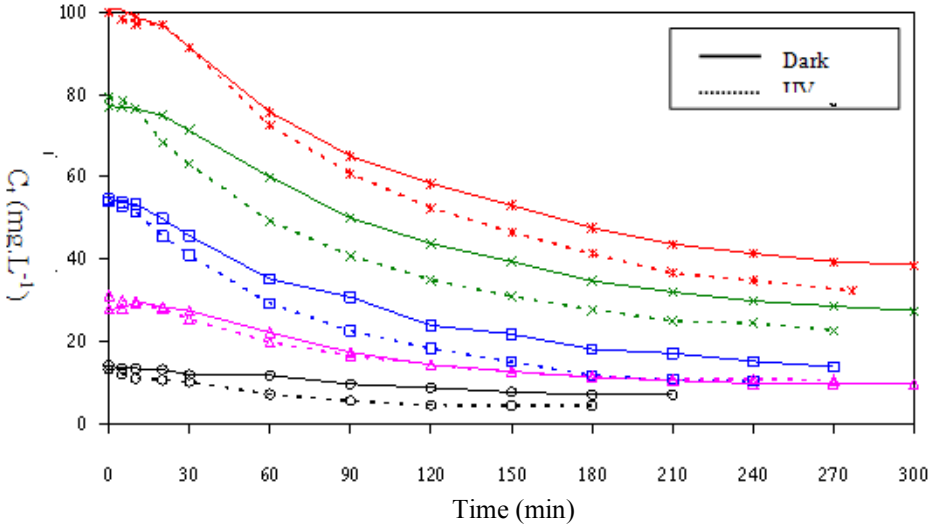

(c)

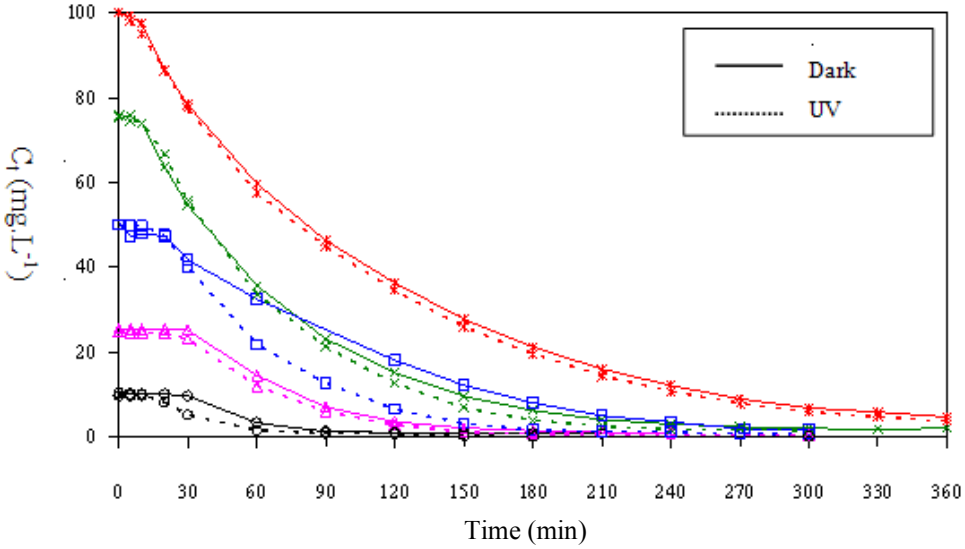

Figure 9. Kinetics of adsorption at various concentration of (a) RR 120 , (b) RY 17, and (c) RB 220: pH = 9, 1 wt% TiO_2 in chitosan film (* C_o = 100 ppm, × C_o = 75 ppm, □ C_o = 50 ppm, Δ C_o = 25 ppm , ○ C_o = 10 ppm)

(a)

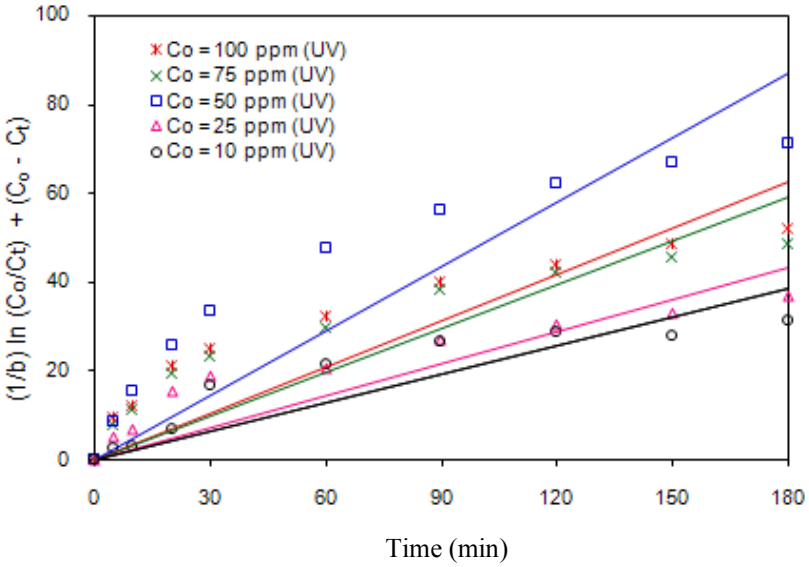

(b)

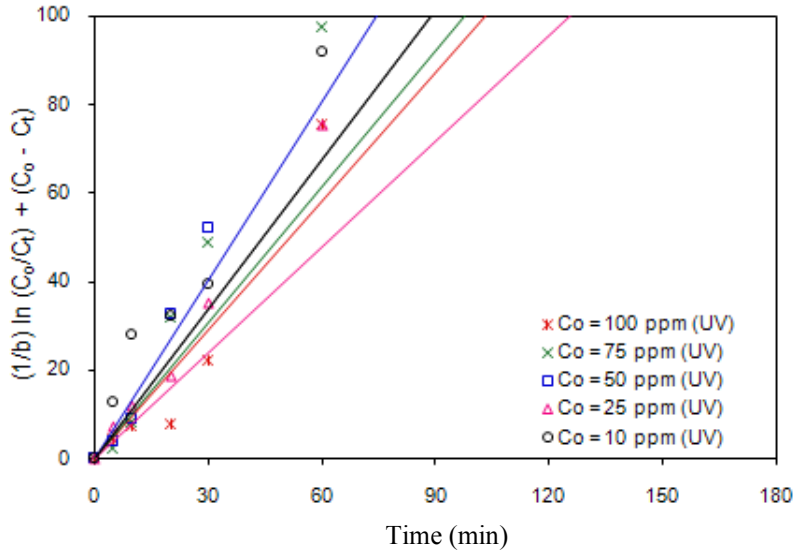

(c)

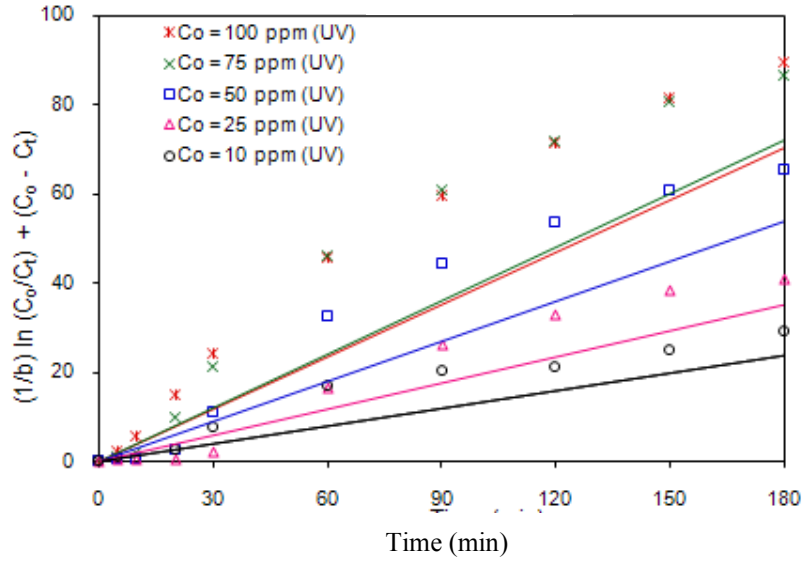

Figure 10. Effect of chitosan-TiO_2 films on dye removal for various type and concentration of dye using Langmuir-Hinshelwood model, (a) RR 120, (b) RY 17, and (c) RB 220

Conclusions

Incorporation of TiO_2 nanoparticle into chitosan film via solution casting method produced the chitosan-TiO_2 film. The immobilized TiO_2 exhibited good distribution in chitosan film when the small amount of TiO_2 was added. The XRD results showed that the crystallinity of chitosan was slightly changed when TiO_2 was added. Fortunately, this disadvantage was overcome by incorporating TiO_2 into the polymer matrix. At higher content of TiO_2, the chitosan-TiO_2 film showed a decrease in tensile stress properties. The use of citric acid as crosslinking agent revealed a good swelling degree due to the presence of –COOH groups. The chitosan-TiO_2 film will be promising sources for photocatalyst materials for various organic compounds in the environment. The thin film catalyst can be easily recycled and suspended in the aqueous solution in order to increase the degree of pollutants removal with TiO_2.

Acknowledgements

The authors thank the Graduate school, Chulalongkorn University for the financial support to P.N. The authors thank the Young Academic Grant, Chulalongkorn University for the financial support to R.N. and K.S**.** Many thanks go to partial support from Inter-Department of Environmental Science, Chulalongkorn University's support on some chemicals, and the Metallurgy and Materials Science Research Institute (MMRI) of Chulalongkorn University for research facilities.

References

1. Shahidi, F., Vidana Arachchi, J.K. and Jeon, Y.J. (1999). Food applications of chitin and chitosan. *Trends Food Sci. Technol.* **10** : 37-51.

2. Guibal, E. (2005). Heterogeneous catalysis on chitosan-based materials : a review. *Prog. Polym. Sci.* **30(1)** : 71-109.

3. Harish P., K.V. and Tharanathan, R.N. (2003). Studies on graft copolymerization of chitosan with synthetic monomers. *Carbohydr. Polym.* **54(3)** : 343-351.

4. He, P., Davis, S.S. and Illum, L. (1999). Chitosan microspheres prepared by spray drying. *Int. J. Pharm.* **187(1)** : 53-65.

5. Gupta, K.C. and Kumar, M.N.V. (2000). Drug release behavior of beads and microgranules of chitosan. *Biomaterials*. **21(11)** : 1115-1119.

6. Berger, J., Reist, M., Mayer, J.M., Felt, O., Peppas, N.A. and Gurny, R. (2004). Structure and interactions in covalently and ionically crosslinked chitosan hydrogels for biomedical applications. *Eur. J. Pharm. Sci. Biopharm.* **57** : 19-34.

7. Zhai, M., Zhao, L., Yoshii, F. and Kume, T. (2004). Study on antibacterial starch/chitosan blend film formed under the action of irradiation. *Carbohydr. Polym.* **57** : 83-88.

8. Fernandez-Saiz, P., Lagaron, J.M. and Ocio, M.J. (2009). Optimization of the biocide properties of chitosan for its application in the design of active films of interest in the food area Publicación. *Food Hydrocolloids.* **23(3)** : 913-921.

9. Garcia, M.A., Pinotti, M., Martino, M. and Zaritzky, N. (2009). Electrically treated composite FILMS based on chitosan and methylcellulose blends. *Food Hydrocolloids.* **23(3)** *:* 722-728.

10. Yang, Y., Zhang, H., Wang, P., Zheng, Q. and Li, J. (2007). The influence of nano-sized TiO_2 fillers on the morphologies and properties of PSF UF membrane. *J. Membr. Sci.* **288(1-2)** : 231-238.

11. Goto, M., Shiosaki, A. and Hirose, T. (1994). Separation of Water/Ethanol Vapor Mixtures through chitosan and cross-linked chitosan membranes. *Sep. Sci. Technol.* **29** : 1915-1923.

12. Enescu, D., Hamciuc, V., Ardeleanu, R., Crista, M., Loanid, A., Harabagiu, V. and Simionescu, B.C. (2009). Polydimethylsiloxane modified chitosan. Part III : Preparation and characterization of hybrid membranes. *Carbohydr. Polym.* **76(2)** : 268-278.

13. Zhang, Z. and Friedrich, K. (2005). Tribological characteristics of micro- and nanoparticle filled polymer composites. In: *Polymer Composites from Nano- to Macro-scale 2005*, New York : Springer : 169-185.

14. Lue, S.J. and Hsieh, S.J. (2009). Modeling water states in polyvinyl alcohol-fumed silica composites. *Polymer*. **50(2)** : 654-661.

15. Depan, D., Kumar, A.P. and Singh, R.P. (2009). Cell proliferation and controlled drug release studies of nanohybrids based on chitosan-g-lactic acid and montmorillonite. *Acta Biomaterialia*. **5(1)** : 93-100.

16. Diebold, U. (2003). The Surface Science of TiO2. Surf. Sci. Rep. **48** : 53-229.

17. Tao, Y.G., Pan, J., Yan, S.L., Tang,B. and Zhu, L.B. (2007). Tensile strength optimization and characterization of chitosan/TiO2 hybrid film. *Mater. Sci. Eng., B.* **138** : 84-89.

18. Kaneko, M. and Okura, I. (2002). *Photocatalysis Science and Technology.* Japan : Kodansha.

19. Zainal, Z., Hui, L.K., Hussein, M.Z., Taufiq-Yap, Y.H., Abdullah, A.H. and Ramli, I. Removal of dyes using immobilized titanium dioxide illuminated by fluorescent. *J. Hazard. Mater.* **125** : 113-120.

20. Crini, G. (2005). Recent Developments in Polysaccharide-Based Materials Used as Adsorbents in Wastewater Treatment. *Prog. Polym. Sci.* **30** : 38-70.

21. Pena, J., Izquierdo-Barba, I., Martinez, A. and Vallet-Regi, M. (2006). New method to obtain chitosan/apatite materials at room temperature. *Solid State Sci.* **8(5)** : 513-519.

22. Wang, T., Turhan, M. and Gunasekaran, S. (2004). Selected properties of pH-sensitive, biodegradable chitosan-poly(vinyl alcohol) hydrogel. *Polym. Int.* **53(7)** : 911-918.

23. Li, J., Chen, Y.P., Yin, Y., Yao, F. and Yao, K. (2007). Modulation of nano-hydroxyapatite size via formation on chitosan-gelatin network film in situ. *Biomaterials*. **28(5)** : 781-790.

24. Tasdelen, B., Kayaman-Apohan, N., Güven, O. and Baysald, B.M. (2005). Anticancer drug release from poly(N-isopropylacrylamide/ itaconic acid) copolymeric hydrogels. *Radiat. Phys. Chem.* **73** : 340-345.

25.Mohan, S.V. and Karthikeyan, J. (1997). Removal of lignin and tannin colour from aqueous solution by adsorption onto activated charcoal. *Environ. Poll.* **97(1-2)** : 183-187.

26. Konstantinou, I. K. and Albanis, T.A. (2004). TiO2-assisted photocatalytic degradation of azo dyes in aqueous solution : Kinetic and mechanistic investigations. *Appl. Catal. B Environ.* **49** : 1-14.